ELSEVIER

New phenolic inhibitors of yeast homoserine dehydrogenase

Linda Ejim,[a] I. Ahmad Mirza,[b] Christina Capone,[a] Ishac Nazi,[a] Steve Jenkins,[a]
Gaik-Lean Chee,[c] Albert M. Berghuis[b] and Gerard D. Wright[a,*]

[a]*Antimicrobial Research Centre, Department of Biochemistry, McMaster University,
1200 Main Street West, Hamilton, ON, Canada L8N 3Z5*
[b]*Departments of Biochemistry, Microbiology and Immunology, McGill University, Montreal, QC, Canada H3G 1Y6*
[c]*Crompton Co./Cie., 120 Huron St., Guelph, ON, Canada N1E 5L7*

Abstract—A relatively unexploited potential target for antimicrobial agents is the biosynthesis of essential amino acids. Homoserine dehydrogenase, which reduces aspartate semi-aldehyde to homoserine in a NAD(P)H-dependent reaction, is one such target that is required for the biosynthesis of Met, Thr, and Ile from Asp. We report a small molecule screen of yeast homoserine dehydrogenase that has identified a new class of phenolic inhibitors of this class of enzyme. X-ray crystal structural analysis of one of the inhibitors in complex with homoserine dehydrogenase reveals that these molecules bind in the amino acid binding region of the active site and that the phenolic hydroxyl group interacts specifically with the backbone amide of Gly175. These results provide the first nonamino acid inhibitors of this class of enzyme and have the potential to be exploited as leads in antifungal compound design.
© 2004 Elsevier Ltd. All rights reserved.

1. Introduction

The amino acid homoserine (Hse) is derived from Asp and is essential for the biosynthesis of the amino acids Met, Thr, and Ile in microbes and plants. The formation of Hse is the branch point where the biosynthetic pathways generating Met or Thr/Ile diverge (Fig. 1), and as such it represents a strategic point for intervention in the development of inhibitors of microbial amino acid biosynthesis. Such inhibitors of fungal Hse biosynthesis have the potential to act as antifungal agents. This hypothesis has been chemically validated by the antifungal agent (*S*)-2-amino-4-oxo-5-hydroxypentanoic acid, which inhibits the Hse biosynthetic enzyme homoserine dehydrogenase (HSD) in a NAD(P)+ dependent manner.[5,14]

HSD reduces aspartate semi-aldehyde (ASA) generating Hse in a nicotinamide cofactor-dependent fashion. Fungal HSD is a homodimer of 38 kDa subunits, unlike the orthologuous enzyme from many bacteria where it is fused to aspartate kinase, the first enzyme in the pathway. The enzyme from the yeast *Saccharomyces cerevisiae* has been expressed, purified, and characterized at the steady state level.[4,6] The 3D-structure of HSD has been determined and it has been demonstrated that this enzyme presents a novel dehydrogenase fold and mechanism.[3] These studies therefore form the basis for further exploration of this enzyme as a target for new antifungal agents.

Here we report the results of a search for inhibitory small molecule ligands of yeast HSD. We have identified
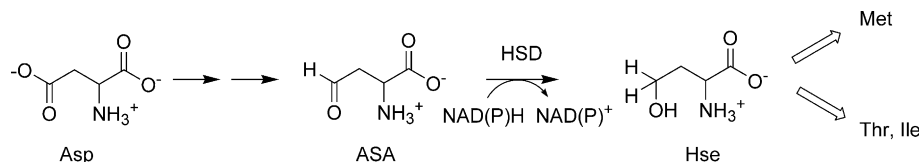

Figure 1. Reaction catalyzed by HSD.

a novel class of inhibitors of fungal HSD and have determined the 3D-structure of one of these in complex with the enzyme. These compounds are the first non-amino acid inhibitors of HSD reported and have the potential to serve as leads in new antifungal drug design.

2. Results and discussion

2.1. Assay development and screen

We elected to measure HSD activity in the forward, NADH oxidizing/ASA reducing, direction and developed an assay suitable for screening in 96 well plates with a screening assay quality coefficient (Z' factor)[15] of 0.76.

A library of 2744 proprietary small molecules, selected on the basis of structural diversity, was screened against purified HSD at 5 μM. This screen revealed four molecules that demonstrated IC$_{50}$ values in the mid to low μM range (Table 1). Compound **1** showed low micromolar IC$_{50}$ for HSD and significant anti-Candidial characteristics (minimal inhibitory concentration (MIC) of 8 μg/mL versus *Candida albicans* and *Candida parapsilosis*). The mode of HSD inhibition of this molecule was therefore further analyzed by steady state kinetics and the compound was found to be an uncompetitive inhibitor of NADH (K_{ii} 24 ± 6 μM) and competitive with ASA (K_{is} 10 ± 2 μM).

A characteristic feature of 3 of 4 of the molecules identified in the initial screen was the presence of a hydroxyl group at position 4 of the ring. A secondary screen of a series of related molecules revealed a new series of bis-sulfanylalkylphenol HSD inhibitors (Table 2). Analysis of the interaction of these molecules with purified HSD demonstrated that enzyme affinity, as assessed by IC$_{50}$, was tolerant of additional bulk in the position *ortho* to the phenol OH, for example, compound **5**. However, affinity generally grew progressively worse with additional alkylation of the ring when compound **5** is compared to **6** and **8**. Increasing the linker length between rings alleviated the lower affinity
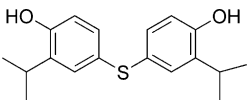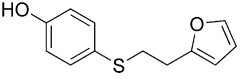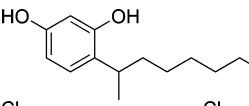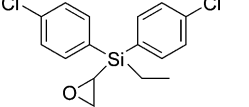
Table 1. Initial hits of HSD screen
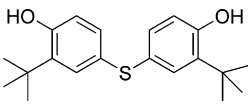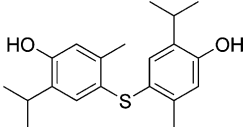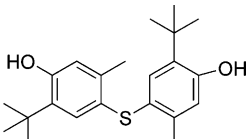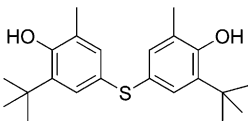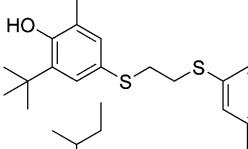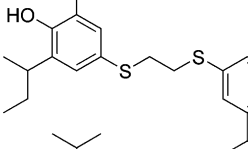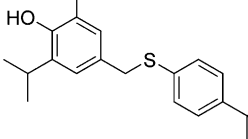
	Compound	IC$_{50}$ (μM)
	1	2.1
	2	5.1
	3	32
	4	26

Table 2. Secondary screen of analogues of compound **1**
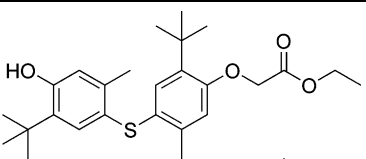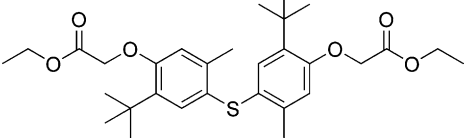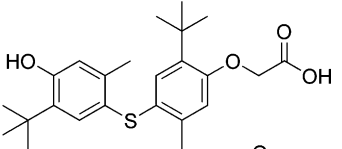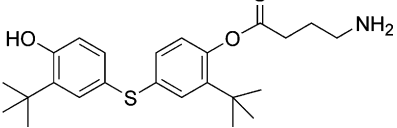
	Compound	IC$_{50}$ (μM)
	5	9.8
	6	40
	7	13.3
	8	70
	9	11
	10	5.9
	11	4.8

(compare **8** with **9** and **10**) and the position of the sulfur atom in respect to the phenolic hydroxyl was not vital to enzyme binding (compound **11**).

The requirement for the symmetrical nature of the compound was probed by ethylcarboxymethylation of compound **7** (Table 3). Enzyme affinity was maintained by monoalkylation of one phenolic OH (**12**) but decreased upon dialkylation of both (**13**). This later compound likely binds in a different fashion to the monophenolic compounds given the structural studies described below. Saponification of **12** gave the acid **14**, which did not show affinity for the enzyme. Derivatization of **5** to give the 4-aminobutyrate derivative **15** did result in a compound that interacted with HSD; however an accurate IC$_{50}$ could not be determined as a result of poor solubility. Therefore, the presence of one free phenolic OH is necessary for HSD inhibition.

We next expanded the series by exploring the importance of alkylation of the aromatic ring with compounds **16–19** (Scheme 1) and none of these showed IC$_{50}$ ⩽ 0.1 mM (limit of solubility). On the other hand, the more soluble cresols **20** and **21** did demonstrate

Table 3. Analysis of nonsymmetrical analogues

	Compound	IC$_{50}$ (µM)
	12	8.2
	13	70
	14	n.i.[a]
	15	n.i.[b]

[a] No inhibition at 50 µM.
[b] <15% inhibition at 50 µM.

some affinity for the enzyme (80% and 10% respective inhibition at 2.5 mM).

In summary, maximal enzyme inhibition activity was observed with phenols alkylated at the *ortho* position and additional alkylation at the *para* position was essential for lowering the IC$_{50}$. The poor inhibition by cresols **20** and **21** with a calculated log$P$ of 2.57, which include the phenol OH group and ring alkylation, and compound **7**, with a calculated log$P$ of 3.36, demonstrates the importance for additional alkylation at the *para* position to increase enzyme affinity (calculated log$P$ of compound **1** is 5.83).

2.2. Biological activity of HSD inhibitors

Compounds **1**, **2**, **3**, **5**, and **6** showed good anti-Candidial activity (MIC between 8 and 32 µg/mL). However

Table 4. MICs of selected compounds in wild-type WT and *HOM6*-deficient (Δ*HOM6*) *S. cerevisiae*

Compound	MIC (µg/mL)			
	YNB medium		RPMI medium	
	WT	Δ*HOM6*	WT	Δ*HOM6*
1	8	8	16	16
2	32	32	32	32
3	32	16	32	32
5	8	8	16	8

the structurally related compounds, for example, **7** and **8**, did not. We further explored the relationship between MIC and HSD inhibition by assessing the inhibition of *S. cerevisiae* BY4742 (ATCC 4040004) and the related strain, *S. cerevisiae* #16933 (ATTC 4016933) in which the gene encoding HSD, *HOM6*, was insertionally inactivated as part of the *Saccharomyces* Genome Deletion Project.[13] This yeast strain is capable of growth on rich medium (Met, Thr, and Ile supplemented) but not minimal media (not shown). The results of these studies are shown in Table 4 and demonstrate that even in the absence of *HOM6*, compounds **1**, **2**, **3**, and **5** retain their antifungal properties, indicating that HSD is likely not the primary cellular target resulting in cessation of growth.

2.3. X-ray analysis

HSD was crystallized in the presence of compound **1** as described in the Experimental section. The location of the binding site of compound **1**, as inferred from the experimental electron density maps, corresponds to the enzyme active site. Modeling of **1** into the HSD active site, based on the X-ray diffraction data, indicated that the molecule binds in the vicinity of the ASA/Hse binding site of each of the monomers of the dimeric enzyme. This is consistent with the observation that **1** is a competitive inhibitor of ASA. Analysis of the data suggests that the predominant interaction constitutes a hydrogen bond between the phenolic OH group of one of the rings and the amide backbone of Gly175 (Fig. 2). The hydroxyl group could also form additional interactions with the amide backbone of Thr176 and the side chain of Asp219. This hydrogen bond network serves to

16   **17**   **18**

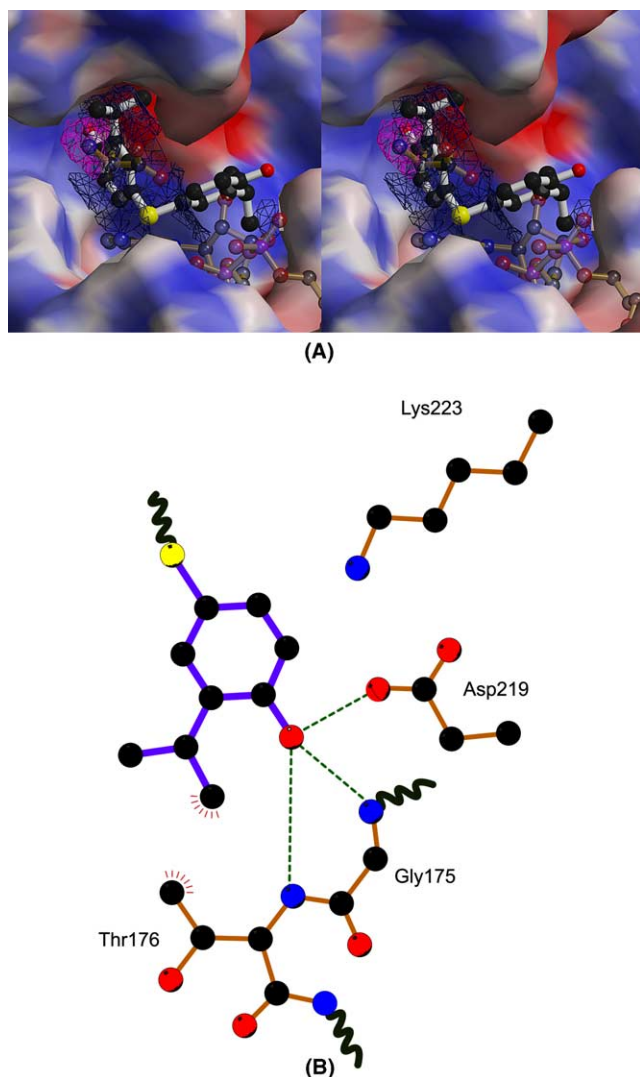**19**   **20**   **21**
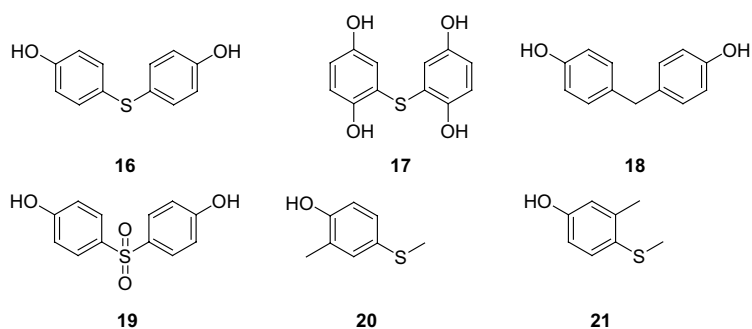
Scheme 1.

Figure 2. X-ray crystal structure of compound **1** bound to HSD. (A) Surface representation of the active site of HSD illustrating the binding site of compound **1** relative to the previously determined substrate and cofactor bind site (PDB 1EBF[3]). The inhibitor is colored gray while the superimposed homoserine and NAD are shown in transparent gold. Also shown is the initial σ_A weight $F_o - F_c$ electron density map contoured at 6σ (magenta) and 2σ (blue). Figure prepared using Molscript,[8] GRASP,[10] and Povscript http://people.brandeis.edu/~fenn/povscript/. (B) Schematic of the interactions between **1** and HSD. Figure prepared with LIGPLOT.[12]

tether the inhibitor in the active site. The experimental density further suggests that the isopropyl moiety located at the *meta* position of **1** makes van der Waals interactions with Cγ of Thr176. However, there is insufficient well-defined density to model the conformation of the entire molecule. This suggests that binding of compound **1** to HSD leaves part of the inhibitor flexible. Most importantly, the X-ray diffraction data suggests that the second ring is likely to occupy multiple conformations in the HSD active site. This mode of **1** binding to HSD provides a rational explanation for the SAR results obtained for close homologues of **1** (i.e., **5–8**). For example, dual *meta* substituted analogues of **1** are not tolerated due to steric clashes with Lys223.

3. Conclusions

We have identified the first nonamino acid inhibitors of the antifungal target HSD. These phenolic molecules have μM affinity for the purified enzyme that can now serve as leads in future campaigns. Cocrystallization of compound **1** and HSD followed by X-ray analysis of the enzyme inhibitor complex has identified key interaction between the phenolic OH and the amide backbone of Gly175 within the amino acid binding region of the enzyme suggests a starting point for further compound design.

4. Experimental procedures

4.1. Materials

Recombinant *S. cerevisiae* HSD was purified as previously described[6] and frozen at −80 °C in aliquots of 1 mg/mL in 10 mM TAPS pH 8.5, 5% (v/v) glycerol. ASA was synthesized as previously described.[6] The 2744 compound library of small molecules (average molecular mass ~400 g/mol) was dissolved in dimethyl sulfoxide. All other chemicals were of reagent grade.

4.2. Synthesis of compounds

Reactions were conducted under a nitrogen atmosphere when anhydrous solvents were used. All ^{1}H NMR spectra were recorded at 200.2 MHz and all ^{13}C NMR were recorded at 50.3 MHz on a Bruker AV-200 spectrometer. Chemical shifts are reported in ppm relative to chloroform and coupling constants are reported in hertz. Electron impact mass spectra were recorded on a Finnigan 4500 quadrapole mass spectrometer and electrospray mass spectra were recorded on a Micromass Quattro-LC triple quadrapole mass spectrometer. Flash column chromatography was performed using silica gel 60 Å from Silacycle (230–400 mesh) and thin-layer chromatography was performed using aluminum backed plates coated with silica gel 60 Å from Machery-Nagel (Alugram®, Sil G/UV$_{254}$, 0.20 mm).

4.2.1. 4-(*tert*-Butoxycarbonylamino)butyric acid. To a solution of 4-aminobutyric acid (1.03 g, 10 mmol) in a solution of *tert*-butanol (20 mL), 1 N sodium hydroxide (10 mL), and water (10 mL) at 0 °C was added di-*tert*-butyl dicarbonate (2.40 g, 11 mmol) in one portion. The mixture was then allowed to stir 3 h at room temperature, during which time the pH was maintained at 9 using 5 N sodium hydroxide. The mixture was then concentrated under reduced pressure to 10 mL and covered with ethyl acetate (30 mL) at 0 °C. The mixture was then acidified (pH 2–3, Congo red indicator paper) with 3 N hydrochloric acid and the organic layer was removed. The aqueous layer was then extracted with ethyl acetate (2 × 30 mL). The combined organic layers were dried (sodium sulfate) and then concentrated under

reduced pressure to afford 4-(*tert*-butoxycarbonyl-amino)butyric acid (1.59 g, 78%) as a clear oil. The clear oil solidified into a white solid upon standing that was used without further purification. ^{1}H NMR (CDCl$_3$, 200 MHz) δ: 10.48 (1H, s), 4.72 (1H, s), 3.17 (2H, m), 2.39 (2H, t, $J = 7.1$ Hz), 1.81 (2H, p, $J = 7.1$ Hz), 1.43 (9H, s); ^{13}C NMR (CDCl$_3$, 50 MHz) δ: 178.3, 156.7, 79.8, 40.0, 31.2, 28.3, 25.1; MS(EI) m/z: 204 [M]$^+$ 148, 147, 130, 129, 115, 102, 86, 59, 57 (base).

4.2.2. 2-*tert*-Butyl-4-(3-*tert*-butyl-4-hydroxyphenylthio)-phenyl 4-(*tert*-butoxycarbonylamino)butanoate. To a solution of 2-*tert*-butyl-4-(3-*tert*-butyl-4-hydroxyphen-ylthio)phenol (300 mg, 0.91 mmol) in dry dichlorome-thane (150 mL) was added 4-(*tert*-butoxycarbonyl-amino)butyric acid (200 mg, 0.99 mmol) and 1-ethyl-3-(3-dimethylaminopropyl)carbodiimide hydrochloride (200 mg, 1.0 mmol) in one portion at 0 °C. The mixture was allowed to stir 30 min before 4-(dimethyl-amino)pyridine (20 mg, 0.16 mmol) was added in one portion. The resultant mixture was then allowed to stir at 0 °C for a further 3 h before being washed with water (2 × 60 mL), brine (80 mL), dried (sodium sulfate), and concentrated under reduced pressure. Flash chroma-tography of the residue on silica gel, using ethyl acetate–hexanes–acetic acid (20:79:1) as eluent, afforded 172 mg 2-*tert*-butyl-4-(3-*tert*-butyl-4-hydroxyphenylthio)phenyl 4-(*tert*-butoxycarbonylamino)butanoate (37%) as a col-orless oil. ^{1}H NMR (CDCl$_3$, 200 MHz) δ: 7.39 (1H, d, $J = 2.2$ Hz), 7.19 (1H, d, $J = 2.1$ Hz), 7.17 (1H, dd, $J = 8.4, 2.2$ Hz), 6.95 (1H, dd, $J = 8.3, 2.1$ Hz), 6.85 (1H, d, $J = 8.4$ Hz), 6.65 (1H, d, $J = 8.3$ Hz), 5.51 (1H, m), 4.66 (1H, m), 3.23 (2H, m), 2.62 (2H, t, $J = 7.3$ Hz), 1.94 (2H, m), 1.45 (9H, s), 1.38 (9H, s), 1.29 (9H, s); ^{13}C NMR (CDCl$_3$, 50 MHz) δ: 176.3, 172.0, 156.3, 155.0, 147.2, 141.5, 137.5, 135.8, 133.1, 132.7, 126.8, 126.2, 124.4, 117.6, 79.8, 40.1, 34.7, 34.5, 32.1, 30.1, 29.4, 28.4, 25.1; MS(ESI) m/z: 514 [M−H$^+$].

4.2.3. 2-*tert*-Butyl-4-(3-*tert*-butyl-4-hydroxyphenylthio)-phenyl 4-aminobutanoate. To a solution of 2-*tert*-butyl-4-(3-*tert*-butyl-4-hydroxyphenylthio)phenyl 4-amino-butanoate (75 mg, 0.15 mmol) in dichloromethane (80 mL) was added trifluoroacetic acid (10 mL). The mixture was allowed to stir 4 h at room temperature before the solvent was removed under reduced pressure. The residue was re-dissolved in dichloromethane (50 mL) and the solvent removed under reduced pressure twice more. Flash chromatography of the residue on silica gel, using methanol–ammonium hydroxide (5:2) as eluent, afforded 47 mg (76%) as a colorless oil. ^{1}H NMR (CDCl$_3$, 200 MHz) δ: 7.72 (3H, m), 7.37 (1H, d, $J = 2.1$ Hz), 7.17 (1H, $J = 2.1$ Hz), 7.09 (1H, dd, $J = 8.4, 2.1$ Hz), 6.88 (1H, dd, $J = 8.4, 2.1$ Hz), 6.75 (1H, d, $J = 8.4$ Hz), 6.62 (1H, d, $J = 8.4$ Hz), 2.94 (2H, m), 2.59 (2H, m), 1.93 (2H, m), 1.34 (9H, s), 1.19 (9H, s); MS(ESI) m/z: 416 [M+H$^+$].

4.3. Small molecule screening of HSD

Primary inhibition screens consisted of 100 μM NADH, 585 μM ASA, approximately 5 μM library compound, 0.02 μg/mL of purified HSD, and 100 mM HEPES pH 7.5 in a final volume of 100 μL in 96 well plates. The reaction was initiated by the addition of HSD and the NADH-dependent reduction of ASA to Hse monitored continuously at 340 nm using a Molecular Devices SpectraMax Plus microtiter plate reader at 25 °C. Compounds demonstrating inhibitory activity were re-screened at 5 μM in duplicate and molecules consistently showing HSD inhibition were confirmed to be concen-tration-dependent inhibitors by the determination of the IC$_{50}$ using Eq. 1.

$$y = \frac{A - D}{1 + \left(\frac{I}{IC_{50}}\right)^S} + D \qquad (1)$$

where $y =$ is the initial rate, A is the minimum response plateau, D is the maximum response plateau, I is con-centration of inhibitor, and S is a slope factor.

Steady state inhibition kinetics were determined using nonlinear least squares fit to Eq. 2 for competitive inhibition, and Eq. 3 for uncompetitive inhibition using the Grafit Ver. 4 software package.[9] The inhibition type was established by inspection of the double reciprocal plots and statistically supported by application of the F-test.

$$v = V_{max}S/(K_m(1 + I/K_{is}) + S) \qquad (2)$$

$$v = V_{max}S/(K_m + S(1 + I/K_{ii})) \qquad (3)$$

4.4. In vitro antifungal activity of compounds

Minimal inhibitory concentrations (MICs) of selected compounds were determined in duplicate over a test range of 0.125–64 μg/mL by broth microdilution meth-ods according to NCCLS guidelines using *C. albicans* ATCC90028 and *C. parapsilosis* ATCC90018. Under the conditions used, the reference drugs amphotericin B and ketoconazole demonstrated respective ranges of 1–4 and 0.004–0.03 μg/mL. MIC values were also obtained against *S. cerevisiae* BY4742 (ATCC 4040004) and a *HOM6* deficient mutant, *S. cerevisiae* #16933 (ATTC 4016933), in the same genetic background. For all MIC studies, the carrier solvent DMSO had no effect on cell growth at the concentrations used.

4.5. X-ray crystallography

HSD for structural studies was obtained as previously described.[2] Purified HSD (10 mg/mL in TAPS pH 8.5 buffer) was incubated overnight with a 5× molar excess of compound **1** and mixed in a 1:1 ratio with a pre-cipitant solution containing either 0.1 M CHES pH 9.5 and 35% PEG 600 or 0.1 M CHES pH 8.5, 40% PEG 400 and 0.2 M NaCl. Five microliter drops were allowed to equilibrate against 0.7 mL of precipitant solution using sitting drop setups. Crystals with dimensions of 0.5 × 0.2 × 0.05 mm were observed after 3 months. Dif-fraction data for several crystals were collected at the X8C beamline of the National Synchrotron Light

Table 5. Structural statistics of the HSD·compound **1** model

Data collection	
Space group	$P2_1$
Unit cell (Å)	$a = 72.5$, $b = 54.3$, $c = 92.5$
	$\beta = 99.0°$
Resolution[a] (Å)	3.0 (3.10–3.00)
Completeness (%)	99.3 (96.3)
Number of reflections	14,617
R_{merge}[b] (%)	8.5 (25.7)
I/σ	7.3
Refinement and model statistics	
R_{cryst}[c] (%)	27.2
R_{free}[d] (%)	35.6
No of atoms[e]	4937
RMSD bonds	0.009
RMSD angles	1.435

[a] Number in parentheses refer to highest resolution shell.

[b] $R_{merge} = \sum |I_i - \langle I \rangle| / \sum I_i$, where I represents the intensities of a multiply measured reflection hkl and $\langle I \rangle$ their average.

[c] $R_{cryst} = \sum |F_o - F_c| / \sum F_o$.

[d] R_{free} is the crystallographic R factor calculated from 9.8% of the data not included in refinement.

[e] Atoms whose occupancy were manually set to zero are excluded from this number.

Source, Brookhaven National Laboratories under cryogenic conditions using a Quantum 4 ADSC CCD detector. Data reduction and scaling were performed with the HKL suite of data processing programs.[11] Statistics pertaining to a dataset obtained from a single crystal that was used for subsequent structure determination are provided in Table 5.

The model of HSD·compound **1** was determined by molecular replacement using the apo form dimer corresponding to chains A and B of the monoclinic HSD structure 1EBU[3] as a search model. Due to the limited resolution of the data, a conservative approach was taken for structure refinement. Only rigid body and minimal positional reciprocal space refinement was performed,[1] and manual interventions, guided by σ_A weighted $F_o - F_c$, $2F_o - F_c$ and simulated annealing omit maps, were essentially restricted to identifying mobile loops whose occupancies were subsequently set to zero.[7] Throughout the refinement process persistent density (greater than 6σ in $F_o - F_c$ maps) was observed in the two active sites of the HSD dimer. Furthermore, this density was also present in an independently determined HSD·compound **1** complex structure using data from a second crystal (3.6 Å resolution). Unfortunately, the density lacked the definition that would allow for the unambiguous modeling of the inhibitor. Most importantly, no density was observed for half of the symmetric compound **1**, suggesting that this moiety is highly mobile. At the very end of refinement, the inhibitor was modeled into this persistent density, taking into consideration possible van der Waals and hydrogen bond interactions and setting the occupancy for half of the symmetric molecule to zero. Statistics pertaining to this structure are listed in Table 5. PDB coordinates and structure factors have been deposited in the Protein Data Bank.

References and notes

1. Brunger, A. T.; Adams, P. D.; Clore, G. M.; DeLano, W. L.; Gros, P.; Grosse-Kunstleve, R. W.; Jiang, J. S.; Kuszewski, J.; Nilges, M.; Pannu, N. S.; Read, R. J.; Rice, L. M.; Simonson, T.; Warren, G. L. *Acta Crystallogr. Sect. D—Biol. Crystallogr.* **1998**, *54*, 905–921.
2. DeLaBarre, B.; Jacques, S. L.; Pratt, C. E.; Ruth, D.; Wright, G. D.; Berghuis, A. M. *Acta. Cryst. Sec. D* **1997**, *D54*, 413–415.
3. De LaBarre, B.; Thompson, P. R.; Wright, G. D.; Berghuis, A. M. *Nat. Struct. Biol.* **2000**, *7*, 238–244.
4. Jacques, S. L.; Ejim, L. J.; Wright, G. D. *Biochim. Biophys. Acta* **2001**, *1544*, 42–54.
5. Jacques, S. L.; Mirza, A.; Ejim, L. J.; Koteva, K.; Hughes, D. W.; Green, K.; Kinach, R.; Honek, J. F.; Lai, H. K.; Berghuis, A. M.; Wright, G. D. *Chem. Biol.* **2003**, *10*, 989–995.
6. Jacques, S. L.; Nieman, C.; Bareich, D.; Broadhead, G.; Kinach, R.; Honek, J. F.; Wright, G. D. *Biochim. Biophys. Acta* **2001**, *1544*, 28–41.
7. Jones, T. A.; Zou, J. Y.; Cowan, S. W.; Kjeldgaard, M. *Acta. Crystallogr. A* **1991**, *47*(Pt 2), 110–119.
8. Kraulis, P. J. *J. Appl. Crystallogr.* **1991**, *24*, 946–950.
9. Leatherbarrow, R. J. *Grafit*; Erithacus Software Ltd: Staines, UK, 2000.
10. Nicholls, A.; Sharp, K. A.; Honig, B. *Proteins* **1991**, *11*, 281–296.
11. Otwinowski, Z.; Minor, W. *Macromol. Crystallogr., Pt A* **1997**, *276*, 307–326.
12. Wallace, A. C.; Laskowski, R. A.; Thornton, J. M. *Protein Eng.* **1995**, *8*, 127–134.
13. Winzeler, E. A.; Shoemaker, D. D.; Astromoff, A.; Liang, H.; Anderson, K.; Andre, B.; Bangham, R.; Benito, R.; Boeke, J. D.; Bussey, H.; Chu, A. M.; Connelly, C.; Davis, K.; Dietrich, F.; Dow, S. W.; ElBakkoury, M.; Foury, F.; Friend, S. H.; Gentalen, E.; Giaever, G.; Hegemann, J. H.; Jones, T.; Laub, M.; Liao, H.; Davis, R. W., et al. *Science* **1999**, *285*, 901–906.
14. Yamaki, H.; Yamaguchi, M.; Suzuki, H.; Nishimura, T.; Saito, H.; Yamaguchi, H. *Biochem. Biophys. Res. Commun.* **1990**, *168*, 837–843.
15. Zhang, J. H.; Chung, T. D.; Oldenburg, K. R. *J. Biomol. Screening* **1999**, *4*, 67–73.